Kinetics of gypsum nucleation and crystal growth from Dead Sea brine

Reznik Itay J. [1,2], Gavrieli Ittai [2] and Ganor Jiwchar [1]

[1] Department of Geological and Environmental Sciences,
Ben-Gurion University of the Negev,
P. O. Box 653, Beer-Sheva 84105,Israel

[2] Geological Survey of Israel,
30 Malkhe Israel,
Jerusalem, 95501

Phone	++972-8-6472-651
Fax	++972-8-6472-997
E-mail	ganor@bgu.ac.il
WEB	http://www.bgu.ac.il/~ganor/

The original publication is available at ScienceDirect:

http://dx.doi.org/10.1016/j.gca.2009.07.018

ABSTRACT

The Dead Sea brine is supersaturated with respect to gypsum (Ω=1.42). Laboratory experiments and evaluation of historical data show that gypsum nucleation and crystal growth kinetics from Dead Sea brine are both slower in comparison with solutions at a similar degree of supersaturation. The slow kinetics of gypsum precipitation in the Dead Sea brine is mainly attributed to the low solubility of gypsum which is due to the high Ca^{2+}/SO_4^{2-} molar ratio (115), high salinity (~280 g/kg) and to Na^+ inhibition.

Experiments with various clay minerals (montmorillonite, kaolinite) indicate that these minerals do not serve as crystallization seeds. In contrast, calcite and aragonite which contain traces of gypsum impurities do prompt precipitation of gypsum but at a considerable slower rate than with pure gypsum. This implies that transportation inflow of clay minerals, calcite and local crystallization of minerals in the Dead Sea does not prompt significant heterogeneous precipitation of gypsum. Based on historical analyses of the Dead Sea, it is shown that over the last decades, as inflows to the lake decreased and its salinity increased, gypsum continuously precipitated from the brine. The increasing salinity and Ca^{2+}/SO_4^{2-} ratio, which results from the precipitation of gypsum, lead to even slower kinetics of nucleation and crystal growth, which resulted in an increasing degree of supersaturation with respect to gypsum. Therefore, we predict that as the salinity of the Dead Sea brine continues to increase (accompanied by Dead Sea water level decline), although gypsum will continuously precipitate, the degree of supersaturation will increase furthermore due to progressively slower kinetics.

1 INTRODUCTION

The Dead Sea is a hypersaline terminal lake located in the Dead Sea Rift valley. The lake's brine has a salinity of about 345 g/l (~280 g/kg) which is about an order of magnitude higher than that of sea water. However, its composition is significantly different from that of evaporated sea water with similar salinity. Relative to evaporated sea water, the Dead Sea brine is enriched in Cl^-, Br^-, Mg^{2+}, Ca^{2+} and K^+ and depleted in Na^+ and SO_4^{2-}. In fact, the concentration of SO_4^{2-} in the Dead Sea is even lower than that in sea water, and it's Ca^{2+}/SO_4^{2-} ratio (115) is therefore extremely high.

Since the 1930s the water level of the Dead Sea has receded dramatically, resulting in a drop of nearly 30 meters. In recent years, in response to increased diversion of freshwater from the lake's drainage basin, the rate of water level drop has accelerated to 1-1.2 m yr^{-1}. This water level decline causes environmental changes in the region, such as receding shorelines, sinkhole formation and changes in the chemical composition of the lake due to evaporation and precipitation of minerals (Gavrieli, 2004).

A comprehensive limnological study of the Dead Sea carried out by Neev and Emery (1967) in the late 1950s up to the early 1960s described massive gypsum precipitation that was occurring from Dead Sea waters during the time. These observations include: (a) ropes left hanging in the water column were coated with gypsum crystals within a period of merely few weeks; (b) gypsum was found in sediment traps; (c) considerable parts of the Dead Sea floor in the littoral zone were covered with gypsum; and (d) suspended gypsum crystals were observed with the unaided eye in water samples. The precipitation of gypsum in the late 1950s is in accord with Stein et al., (1997) who suggested that during periods of negative water

balance massive gypsum precipitation occurred in the Dead Sea and its Late Pleistocene precursor, Lake Lisan. However, by the early 1980s, gypsum accumulation rates were lower by three orders of magnitude compared to the rates recorded by Neev and Emery (1967) even though the negative water balance continued and even worsened (Levy, 1987). The reduction in gypsum accumulation rates may be attributed to the reduction in the natural supply of SO_4^{2-} due to the diversion of freshwater from the lake.

By the early 1980s, the Dead Sea has evaporated to the point that halite (*NaCl*) started to precipitate (Steinhorn, 1983). Since then, it is the major precipitate from the Dead Sea, and the phenomena described by Neev and Emery (1967) for gypsum are presently observed with halite (Gavrieli, 1997). It was suggested that even if gypsum precipitation still occurs in the Dead Sea it is masked by the higher quantities of precipitated halite (Herut et al., 1998).

In addition to the precipitation in the Dead Sea itself, halite and gypsum also precipitate in the artificial evaporation ponds constructed at the southern basin of the Dead Sea by the chemical industries. Further evaporation of the brine leads to precipitation of carnallite ($KMgCl_3 \cdot 6H_2O$) which is harvested for the production of potash. The residual concentrated brine is then returned to the Dead Sea.

Thermodynamic calculations based on Pitzer's equations (Krumgalz and Millero, 1982; Krumgalz, 2001) show that despite the fact that gypsum precipitates in the Dead Sea, the brine remains supersaturated with respect to gypsum (Katz et al., 1981; Krumgalz and Millero, 1983; Gavrieli, 1997; Krumgalz, 1997). Currently, the degree of saturation with respect to gypsum (DSG) is 1.42±0.08. The Dead Sea brine is also supersaturated (degree of saturation, $\Omega>1$) with respect to other SO_4^{2-} minerals, including anhydrite ($CaSO_4$, Ω=1.94), barite ($BaSO_4$, Ω=11.75) and celestite

($SrSO_4$, Ω=2.48). In contrast to the above SO_4^{2-} phases, which maintain high supersaturation in the Dead Sea brine, halite remains close to saturation, ($1 \leq \Omega < 1.1$ (Gavrieli, 1997)).

The two basic processes of precipitation of minerals are: (1) *nucleation*, by which a new phase is formed and (2) *crystal growth* during which the formed nuclei and crystals continue growing. Most of the previous studies of gypsum nucleation and crystal growth focused on industrial needs, where gypsum is usually an unwanted scale deposit. Therefore, these studies focused on gypsum precipitation from solutions with relatively low ionic strength, similar to the conditions in the industry (Edinger, 1973; Van Rosmalen et al., 1981; Christoffersen et al., 1982; Cody and Cody, 1989). Most of these studies were conducted in solutions that contain equivalent concentrations of Ca^{2+} and SO_4^{2-} (Liu and Nancollas, 1970; Smith and Sweett, 1971; Gill and Nancollas, 1979; Kagawa et al., 1981; Van Rosmalen et al., 1981; Christoffersen et al., 1982; Witkamp et al., 1990; He et al., 1994b). The few studies that examined gypsum nucleation and crystal growth in high ionic strength conditions, did so in solution of ionic strength of only up to 6 *m* (mol kg H_2O^{-1}) (He et al., 1994a; He et al., 1994b), which is still significantly lower than the ionic strength of the Dead Sea brine (10 *m*).

1.1 The effect of evaporation and consequential precipitation on precipitation kinetics

The kinetics of both nucleation and crystal growth depend on numerous parameters, some of which are common to both. As a supersaturated solution evaporates and minerals precipitate, the solution's chemistry, thermodynamic state and precipitation kinetics are altered. During evaporation, the concentrations of the dissolved ions increase, including the concentrations of the dissolved lattice ions and

possible catalysts and inhibitors. Precipitation on the other hand leads to decrease in the concentrations of the dissolved lattice ions and may change their respective ratio in the solution. Figure 1 schematically illustrates the affects of evaporation and consequent mineral precipitation on the ionic strength, activity coefficients of the free ions, formation of aqueous complexes, concentrations of lattice ions and lattice cation/anion ratio and the resulting impacts on both degree of saturation and mineral solubility. Mineral solubility may be defined as the molal concentration of a mineral that is dissolved in a solution at saturation. For stoichiometric solutions, the solubility is equal to the molal concentration of any of the lattice ions, divided by its coefficient in the mineral formula. For non-stoichiometric solutions the solubility is equal to the lowest amongst these quotients. Accordingly, maximal solubility (at a given ionic strength and composition) is attained when the ratio between the dissolved lattice ions equals that of the mineral. It follows that in the SO_4^{2-}-depleted Dead Sea brine, gypsum solubility is defined as the concentration of SO_4^{2-} at which the brine is saturated with respect to gypsum.

Following evaporation, the increase in total concentration of the dissolved ions leads to the formation of aqueous complexes, which may include the mineral lattice ions, thereby increasing solubility and decreasing the degree of saturation (Fig. 1). At low ionic strengths (up to ~1 *m*), activity coefficients of the free ions (including lattice ions) decrease with increasing salinity. This leads to increase in solubility and decrease in the degree of saturation of the mineral. Therefore, up to an ionic strength of 1 *m* the effects of formation of aqueous complexes and variation in activity coefficients are similar. At higher ionic strengths (>1 *m*) activity coefficients generally increase with increasing salinity, thereby decreasing the solubility and

increasing the degree of saturation. Accordingly, at I>1 *m* the impact of ion complexes on solubility counteracts that of increasing activity coefficient.

It is widely argued that higher solubility allows more impinging growth units which results in faster precipitation kinetics (Brandse et al., 1977; Witkamp et al., 1990; Zhang and Nancollas, 1992; Bosbach et al., 1996; Sheikholeslami and Ong, 2003). Specifically, gypsum nucleation and crystal growth kinetics was shown to positively correlate with solubility both when the solubility is altered by increasing the ionic strength of the solution (He et al., 1994a; He et al., 1994b) and by changing the Ca^{2+}/SO_4^{2-} ratio (Zhang and Nancollas, 1992; Alimi and Gadri, 2004).

Another effect which influences crystal growth rate by retarding the precipitation kinetics is adsorption of background electrolytes onto the forming mineral. For example, Zhang and Nancollas (1992) suggested that Na^+ and to a lesser extent K^+, adsorb onto the surface of gypsum, partially inhibiting its growth rate. As salinity increases, adsorption may increase due to increased concentration, thereby decreasing the precipitation rate.

Since most of the relationships presented in Fig. 1 between the various variables and precipitation kinetics are interrelated and occur simultaneously with evaporation and consequential precipitation, it is presently impossible to differentiate and quantify the relative impact of each variable. Therefore, it is not possible to predict a-priori the overall effect of evaporation and precipitation on gypsum precipitation kinetics from Dead Sea brine.

The aim of the current study is to quantify, by combining laboratory experiments, theoretical geochemical models and chemical data obtained from historic and present measurements, the different parameters affecting the kinetics of gypsum nucleation and crystal growth in the Dead Sea. This will enable us to

understand why the Dead Sea has remained supersaturated with respect to gypsum for at least several decades and predict how the Dead Sea will evolve with respect to gypsum in the future, if left to evaporate.

2 MATERIALS AND METHODS

2.1 Dead Sea Brine

Dead Sea brines were collected from various locations in the northern basin of the Dead Sea. The brines were pumped from a depth of approximately 4 meters. The collected brines were held in closed containers at room temperature (20-30˚C) for several months. During this period, halite precipitated in the containers, probably due to changes in solubility of the brine as a result of the temperature changes. Analyses of SO_4^{2-} concentrations close to the date of sampling and two months thereafter show no difference (within measurement error) suggesting that gypsum did not precipitate in the containers. Before introducing it into an experiment, the brine was filtered through a 0.45μM Durapore membrane (milipore). Table 1 shows the average chemical composition and DSG of the Dead Sea brines used in the experiments.

2.2 Experimental setting

2.2.1 Batch experiments:

Seeded batch experiments were carried out in 60 ml Teflon bottles, fully immersed in a thermostatic water-bath held at a constant temperature of 25±0.1ºC. The batch experiments were shaken once a day. Periodically, a 1 g sample was taken using a syringe, filtered with a 0.45 μM filter disk and diluted for chemical analysis.

2.2.2 Flow-through experiments:

Experiments were carried out using stirred-flow reaction cells (ca. 35 ml) fully immersed in a thermostatic water-bath held at a constant temperature of 25.0±0.1ºC

(Fig. 2). The reactors were composed of two chambers, a lower chamber of 33mm inner diameter and an upper chamber of 26 mm inner diameter. The two chambers were separated by a fine 5 μm nylon sieve. A submersed stir-plate controlled two Teflon-coated stir bars. The first was mounted on the bottom of the cell and the second was placed on the fine 5 μm mesh to improve the stirring of the upper cell. In most of the experiments crystallization seeds were placed on the 5 μm mesh. The sieve prevented the falling of the crystallization seeds to the lower chamber. The inlet of the inflow Dead Sea brine was located at the lower chamber, while the outlet was located in the upper chamber. A 0.45 μm mesh was mounted at the top of the cell in order to prevent crystals from exiting the system. Flow rates were controlled by peristaltic pumps. In any one run, the flow rate was held constant for a long enough time for steady-state conditions to be closely achieved. Steady states were defined to have been achieved when a series of outflow SO_4^{2-} concentrations remained constant (± 5%). After steady-state conditions were reached, precipitation rates were evaluated. Most of the experiments consisted of one stage, i.e., the experiment was stopped after steady state was approached.

2.3 Seed Material

Various minerals, most of which are naturally transported to or precipitate in the Dead Sea, were used as seeds in the experiments, including gypsum, clay minerals (montmorillonite and kaolinite), calcite and aragonite. These minerals were cleaned, ground and sieved to retain a particle size fraction of 53-149 μM.

Gypsum crystal seeds were prepared from natural occurring selenite (gypsum) collected from Machtesh Ramon in the Negev desert, Israel. X-ray diffraction (XRD) of the clean sample showed no other mineral phases. Accordingly, chemical analysis of the dissolved gypsum indicated that it contains only minor concentrations (<0.2%) of elements other than Ca^{2+} and SO_4^{2-}. Montmorillonite sample SAZ-1 and kaolinite sample KGa-1b are international reference samples of the Clay Mineral Society

Source Clay Repository. SAZ-1 contains considerable amounts of silica phases (quartz, cristobalite and/or amorphous silica) and minor quantities of alkali-feldspars, plagioclase and carbonates (Metz et al., 2005). KGa-1b is an almost pure well-ordered kaolinite, with a trace abundance of anatase (Pruett and Webb, 1993). Calcite idiomorphic crystal obtained from Ward's Natural Sciences was found to contain some quartz and gypsum impurities (<0.3%). Aragonite-rich sediments deposited by Lisan Lake, the Late Pleistocene precursor of the Dead Sea, were collected from the Lisan Formation near Massada, Dead Sea, Israel. The sediments contain mostly aragonite with some quartz, calcite and gypsum impurities (Torfstein et al., 2008).

2.4 Analyses

Density of the inflow and outflow solutions was measured with a Paar digital DMA-35 density meter. The uncertainty in the density measurement was ±0.0005 g cm^{-3}.

SO_4^{2-} was analyzed using a Dionex's DX500 high pressure liquid chromatography. Eluent solution containing 1.8 mM Na_2CO_3 and 1.7 mM $NaHCO_3$ is pumped through a guard column (AG4A-SC) and an anion column (AS4A-SC) at a flow rate of 2 ml/min. Approximately 5 ml of diluted Dead Sea solution (1:100) is injected using an auto-sampler into a 25 µl feeding loop. Based on repeated analyses of SO_4^{2-} standards, we estimate the precision to be ± 3% (1 standard deviation).

Na^+, K^+, Ca^{2+}, Mg^{2+}, Ba^{2+} and Sr^{2+} were analyzed using Inductively Coupled Plasma Atomic Emission Spectroscopy (ICP-AES). Cl^- and Br^- combined were measured by a potentiometeric titration method, using a silver and calomel electrodes with $AgNO_3$ as the titrant. Br^- was then measured by Inductively Coupled Plasma Mass Spectrometry (ICP-MS) which enables the derivation of Cl^- alone. The precision of the analysis of all the major elements except SO_4^{2-} is ±2%.

The specific surface area of the gypsum was measured by the Brunauer-Emmett-Teller (BET) method (Brunauer et al., 1938), using 5-points of N_2 adsorption

isotherms, with a Micromeritics Gemini II-2375 surface area analyzer. BET surface area was determined after an outgassing period of ten days at a temperature of 40ºC. The relatively low temperature for the outgassing procedure was selected in order to avoid dehydration of gypsum and transformation into bassanite or anhydrite (Billo, 1986; Deutsch, 1994). The BET-determined initial specific surface area of the gypsum seeds used for the experiments is 0.41±0.06 m^2 g^{-1}. The mineralogical compositions of the seeds were characterized by X-ray diffraction (XRD) using a Philips PW1700 diffractometer.

3 CALCULATIONS

3.1 Gypsum precipitation kinetics

Gypsum precipitation and dissolution reaction is expressed by:

$$(1) \qquad CaSO_4 \cdot 2H_2O \Leftrightarrow Ca^{2+} + SO_4^{2-} + 2H_2O \,.$$

In a well-mixed flow-through system where gypsum precipitates, the change in concentration of the products with time (mol kg solution^{-1} s^{-1}), is obtained from the following mass balance equation:

$$(2) \quad \frac{dC_{j,out}}{dt} = -Rate \cdot \nu_j \cdot \frac{S_r}{V \cdot \rho} - \frac{q}{V \cdot \rho}(C_{j,out} - C_{j,in}) \,,$$

where $C_{j,in}$ and $C_{j,out}$ are the concentrations of component j (SO_4^{2-} or Ca^{2+}) in the inflow and the outflow solutions (mol kg solution^{-1}) respectively; ν_j is the stoichiometry coefficient of j in the precipitation reaction; *Rate* is the precipitation rate (mol m^{-2} s^{-1}); t is time (s); S_r is the overall surface area of the mineral (m^2); V is the volume of the cell (m^3) and q is the fluid weight flux through the system (kg s^{-1}). Note that in this formulation, the rate is defined to be positive for precipitation and negative for dissolution.

Rearranging Eq. (2) gives:

$$(3) \quad Rate \cdot \nu_j = -\frac{dC_{j,out}}{dt} \cdot \frac{V \cdot \rho}{S_r} - \frac{q}{S_r}(C_{j,out} - C_{j,in}) .$$

Under steady state conditions, when the composition of the outflow solution reaches a constant value, i.e. $\left(\frac{dC_{j,out}}{dt} = 0\right)$, the precipitation rate may be obtained as follows:

$$(4) \quad Rate \cdot \nu_j = -\frac{q}{S_r}(C_{j,out} - C_{j,in}) .$$

In the seeded experiments, gypsum growth was small relative to the original seeding and therefore did not considerably affect the available surface area.

3.2 Gibbs free energy

The deviation from equilibrium with respect to gypsum precipitation is calculated in terms of the Gibbs free energy (ΔG_r):

$$(5) \quad \Delta G_r = RT \ln\left(\frac{IAP}{K_{eq}}\right) = RT \ln(DSG) ,$$

where R is the gas constant (J K^{-1} mol^{-1}); T is the temperature (K); IAP and K_{eq} are the ion activity product and the thermodynamic solubility product, respectively, and DSG is the degree of saturation with respect to gypsum.

Taking the activity of the reactant solid gypsum in Eq. (1) to be 1, the ion activity product of the precipitation reaction is:

$$(6) \quad IAP = \frac{a_{Ca^{2+}} \cdot a_{SO_4^{2-}} \cdot a_{H_2O}^2}{1} ,$$

where a_i is the activity of constituent i. The activities are strongly dependent on the composition and ionic strength of the solution. In the present work they are calculated, along with the DSG values, using Pitzer's approach provided by the

PhreeqC code (Parkhurst and Appelo, 2007). Reznik et al. (2009) showed experimentally that the PhreeqC code correctly calculates the DSG values in Dead Sea brine, despite their unique composition and extremely high ionic strength. The uncertainty in the calculated DSG for the Dead Sea brine is ±8% (1 standard deviation). This uncertainty is derived from the analytical uncertainties of the different ions used to calculate DSG.

4 RESULTS AND DISCUSSION

Eleven flow-through experiments were conducted (Table 2). Residence time of the solutions in contact with the crystals ranged between 6-14 hours. The precipitation rates presented in Table 2 were calculated according to Eq. (4). In order to allow a longer residence time, six long term (~100 days) batch experiments were conducted, using the same Dead Sea brine sample. The SO_4^{2-} concentration of the Dead Sea brine sampled was 3007±27 μmol kg solution^{-1} (n=12) and its initial DSG was calculated to be 1.36±0.11 (Table 3).

4.1 Impact of crystallization seeds on gypsum precipitation

4.1.1 Gypsum seeding and control (no seeding) experiments

SO_4^{2-} concentrations in the inflow and outflow solutions of two flow-through experiments performed with a relatively high amount of gypsum crystallization seeds (2 g, experiment AN) and with no crystallization seeds (experiment AO), are shown in Fig. 3. No change in the brine's chemical composition was detected in the experiment with no seeding, whereas the decrease in SO_4^{2-} concentration in the

seeded experiment testifies to gypsum precipitation in the presence of crystallization seeds.

The same experimental concept was repeated using a batch apparatus (Fig. 4). Less than 24 hours after the introduction of gypsum crystals, the brine reached equilibrium (DSG=1.00±0.08). This shows that when enough gypsum crystallization seeds are present, the brine reaches equilibrium within a short time. In the control experiment (no seeding), a change in SO_4^{2-} concentration was observed after about 80 days, indicating that gypsum nucleation from Dead Sea brine is very slow. The control experiment remained supersaturated with respect to gypsum even after more than 100 days.

4.1.2 Seeding experiments with minerals other than gypsum

In order to examine if other minerals may serve as crystallization seeds for the precipitation of gypsum from Dead Sea brine, a set of flow-through experiments were conducted containing various other potential crystallization seeds (Table 2). In all flow-through experiments with minerals other than gypsum, the difference between the inflow and outflow SO_4^{2-} concentrations ($\Delta_{sulfate}$) was less than the analytical uncertainty (~±50 μmol kg solution^{-1}). These observations indicate that gypsum precipitation did not occur during the course of the flow-through experiments that contained minerals other than gypsum (within analytical limitations).

In the batch experiments (Fig 4), no difference was found between the control experiment and experiments conducted with montmorillonite and kaolinite, indicating that these minerals do not prompt precipitation of gypsum. A change in composition was noticed when calcite and aragonite were added. However, these minerals were found to contain gypsum impurities which probably prompted the precipitation. As calcite was reported by Gill and Nancollas (1979) to be a suitable substrate for

gypsum, heterogeneous growth on calcite may be an alternative reason to explain the decrease in SO_4^{2-} in this experiment (Fig 4).

The fact that gypsum precipitation was noticed in the batch experiments that included the calcite and aragonite and not in the flow-through experiments is attributed to difference in the residence times of the solutions. It follows that the rate of gypsum precipitation in experiments conducted with minerals other than gypsum is immeasurable for short residence times such as that in the flow-through experiments.

4.2 Parameters affecting heterogeneous crystal growth rates

Since crystal growth is a surface reaction, the precipitation rate depends on the surface area:

$$(7) \quad Rate_{het} = k'_{het} \cdot S_r = k'_{het} \cdot S_s \cdot m \,,$$

where $Rate_{het}$ is the heterogeneous crystal growth rate (mol s^{-1}); k'_{het} is an apparent heterogeneous rate constant (mol s^{-1} m^{-2}); S_r is the total reactive surface area (m^2); S_s is the specific surface area (m^2 g^{-1}) and m is the mass of gypsum (g). Rearranging Eq. (7) while taking into account that the apparent heterogeneous rate constant depends on the degree of deviation from equilibrium, gives:

$$(8) \quad \frac{Rate_{het}}{S_s \cdot m} = k_{het} \cdot f(\Delta G_r) \,,$$

where k_{het} is the heterogeneous rate constant (mol s^{-1} m^{-2}) and $f(\Delta G_r)$ is a function describing the dependency of the growth rate on deviation from equilibrium.

When crystal growth or dissolution involves surface defects, the function $f(\Delta G_r)$ takes the typical form (Lasaga, 1998):

$$(9) \quad f(\Delta G_r) = \left(\exp\left(\frac{\Delta G_r}{RT} \right) - 1 \right)^n = (DSG - 1)^n \,,$$

where n is the apparent reaction order with respect to the deviation from equilibrium (*DSG-1*). Merging Eq. (9) and Eq. (8) yields the following expression which describes the normalized heterogeneous growth rate:

$$(10) \quad \frac{Rate_{het}}{S_s \cdot m} = k_{het} \cdot (DSG - 1)^n .$$

Equations (9) and (10) apply for solutions in which the dissolved lattice activity ratios are similar to the stoichiometries of the precipitating minerals. A more rigorous rate equation for crystal growth, which applies for both stoichiometric and non-stoichiometric solutions was shown by Nielsen (1981):

$$(11) \quad \frac{Rate_{het}}{S_s \cdot m} = k''_{het} \cdot (DSG^{1/\upsilon} - 1)^n ,$$

where υ is the number of molecules in a formula unit of the crystal, other than the solvent (two in the case of gypsum). For stoichiometric solutions, k_{het} in the rate law of Eq. (10) is linearly proportional to k''_{het} in Eq. (11).

The Burton Cabrera and Frank (BCF) crystal growth theory (Burton et al., 1951) calculates the balance between the attachment and detachment of molecules (adatoms) on the mineral surface during a spiral growth of a step, which is initiated by a screw dislocation. According to the BCF theory n=2 for spiral growth (Lasaga, 1998).

Experimental studies showed that the bulk growth rate of gypsum (the sum of growth on all crystallographic surfaces) at low ionic strength solutions with small deviation from equilibrium (low degrees of supersaturation) is a second order reaction (n=2) (Liu and Nancollas, 1970; Liu and Nancollas, 1973; Christoffersen et al., 1982; Amjad, 1985; Witkamp et al., 1990). For higher degrees of supersaturation, the order of the crystal growth reaction increases up to 3.5 (Brandse et al., 1977). The reaction

order may be affected by background electrolytes as well: in solutions containing $NaNO_3$ (1 mol kg solution^{-1}) the reaction order increases with increasing supersaturation (Witkamp et al., 1990). However, other electrolytes, such as NaCl (up to 6 *m*), have no effect on the order of gypsum growth rate and it remains a second order reaction (He et al., 1994b). Although most overall growth rate studies describe a second order reaction, several microscopic studies show no evidence for spirals on the dominant surface (Van Rosmalen et al., 1981; Bosbach and Rammensee, 1994; Hall and Cullen, 1996). Thus, an alternative mechanism was suggested by which gypsum grows in a layer-by-layer mechanism, which may also account for a second order reaction (Goto and Ridge, 1967; Van Rosmalen et al., 1981; Bosbach and Rammensee, 1994).

In order to examine if the variation of gypsum crystal growth rates from Dead Sea brine may also be described by a second order reaction, we plotted our experimental flow-through steady-state rates (Table 2) vs. $DSG^{1/2}$-1 (Fig. 5). By assuming n=2 and ν=2 in Eq. (11), we fitted the experimental data, determined k''_{het} and obtained the following rate law:

$$(12) \qquad Rate_{het} = (1.05 \pm 0.05) \cdot 10^{-6} (DSG^{1/2} - 1)^2 \ mol\ m^{-2}\ s^{-1}.$$

The results indicate that the overall data fits excellently with a second order dependency (dotted curve in Fig. 5), as predicted by both the BCF theory and a layer-by-layer mechanism. However, it is important to note that different combinations of n and k''_{het} in Eq. (11) can yield other curves that adequately describe the experimental data. In other words, the second order rate law (Eq. (12)) is not unique, and other rate laws may be applied as well (Nancollas, 1979).

4.3 Nucleation and crystal growth kinetics from Dead Sea brine

In the control batch experiment (Fig. 4), decrease in the SO_4^{2-} concentration of the Dead Sea brine was first detected only after approximately 80 days. In contrast, in solutions of much lower ionic strength but with similar degrees of supersaturation such a change occurs within a much shorter time scale, ranging from a few hours (Packter, 1974; Lancia et al., 1999; El-Shall. et al., 2002) to a day (He et al., 1994a). A similar trend is shown for crystal growth rates. A comparison of the crystal growth rates of gypsum from Dead Sea brine with the results of Zhang and Nancollas (1992) who conducted crystal growth experiments using synthetic NaCl solutions at much lower ionic strength solutions, reveal that for the same degrees of supersaturation, the precipitation rate (mol s^{-1} m^{-2}) from Dead Sea brine is slower by at least one order of magnitude.

We suggest that the slow nucleation in the Dead Sea brine is due to the low solubility which derives from the high Ca^{2+}/SO_4^{2-} ratio and high ionic strength. In pure water, gypsum solubility is ~15500 μm (Ca^{2+}/SO_4^{2-} = 1:1), while in the Dead Sea brine, gypsum solubility is only ~3200 μm. The low solubility leads to an increased interfacial energy and to a slow rate of nucleation. The low solubility also leads to a reduced rate of crystal growth. The rate of crystal growth is also reduced due to the inhibitory effect of Na^+. Furthermore, lack of suitable crystallization seeds prevents crystal growth from taking place, thereby forcing the system to be limited by the rate of nucleation and suspension time of the crystals in the brine. Elaboration on the effects of each parameter is given below.

4.3.1 Interfacial energy effect on nucleation

According to the classic nucleation theory, the induction time (t_{ind}) for the formation of a critical nucleus in a system is described by (He et al., 1994a):

$$\log\ t_{ind} = \frac{B}{(Log\ DSG)^2} - C, \quad (13)$$

where C is a constant and B is defined as:

$$B = \frac{\beta\sigma^3 V_m{}^2 N_A f(\vartheta)}{(2.3RT)^3}, \quad (14)$$

where β is a geometric factor (16π/3 for a spherical nucleus), σ is the interfacial tension between the crystal and the aqueous solution (J m^{-2}), V_m is the molar volume of gypsum (74.69 cm^3 mol^{-1}), N_A is Avogadro's number, $f(\vartheta)$ is the correction factor for heterogeneous nucleation (0.01 for heterogeneous nucleation and 1 for homogeneous nucleation). The interfacial tension is related to the solubility (Nielsen and Sohnel, 1971; Sohnel, 1982):

$$\sigma = -A\ \log C_s + F, \quad (15)$$

where A (J m^{-2} m^{-1}) and F (J m^{-2}) are constants for a specific solution and C_s (m^{-1}) is the mineral's solubility.

According to Eq. (15), as solubility decreases, the interfacial tension (σ) increases. A higher σ poses a high energetic barrier, thereby reducing the statistical chance for the creation of a stable nucleus. This leads to a longer induction time and a slower nucleation rate.

4.3.2 *The effects of ionic strength, Ca^{2+}/SO_4^{2-} ratio and Na^+ concentration on crystal growth rates*

As discussed in the introduction, increasing the ionic strength in high ionic strength solutions reduces the solubility, which results in slower kinetics. In addition, Zhang and Nancollas (1992) showed that at a given degree of saturation (DSG=1.69), gypsum precipitation rate from 1 *m* NaCl solutions decreases linearly with increasing log of Ca^{2+}/SO_4^{2-} (Fig. 6). Thus, the rate of crystal growth is not merely a function of the thermodynamic driving force, but also depends upon the relative concentration and characteristics of the individual ions. Moreover, Zhang and Nancollas (1992), suggested that Na^+, and to a lesser extent K^+, adsorbs onto the surface of gypsum, partially inhibiting its growth rate. Despite the differences in compositions between Dead Sea brine and the NaCl solutions that Zhang and Nancollas (1992) worked with, gypsum precipitation rate from Dead Sea brine (corrected to DSG=1.69 according to Eq. (12)) agrees well with the extrapolation of Zhang and Nancollas's (1992) data (triangle in Fig. 6). Based on this extrapolation, we suggest that the main parameters that retard the rate of crystal growth in Dead Sea brine is the high Ca^{2+}/SO_4^{2-} ratio and high Na^+ concentration.

4.3.3 *Lack of available crystallization seeds*

Heterogeneous precipitation rate is limited by the nucleation rate. However, if suitable crystallization seeds are introduced, heterogeneous precipitation will be promoted. Previous studies found that anhydrite, hemihydrate, gypsum, barite and calcite substrates encourage heterogeneous precipitation of gypsum (Gill and Nancollas, 1979; Kagawa et al., 1981). In this study precipitation of gypsum was promoted by the presence of calcite and aragonite. However, these phases were found

to contain gypsum impurities. Nevertheless, despite the very high seed/brine ratio, the solution remained supersaturated even after 4 months, probably due to a limited available surface area of gypsum in these samples. Thus, neither calcite nor aragonite is as favored as pure gypsum.

We conclude that in the Dead Sea nucleation rates of gypsum are slow and that natural transported sediments (air borne dust and detritus) are not suitable for serving as efficient crystallization seeds. Since the Dead Sea remains supersaturated with respect to gypsum we assume that both these processes have little impact on the Dead Sea's chemistry. Therefore, we suggest that the relatively few nuclei that do form in the Dead Sea, grow relatively fast and due to crystal size, settle rapidly to the sea floor, where they are buried and do not continue to serve as crystallization seeds. Since the nucleation rate is slower relatively to the crystal growth rate, at any given time the water body contains limited amount of gypsum crystals. It follows that both the in situ formation and the external transport of surfaces on which gypsum can grow is insufficient to promote enough gypsum precipitation to decrease gypsum supersaturation in the Dead Sea.

4.4 Precipitation of gypsum in the Dead Sea, past, present and future

Since the Dead Sea is a terminal lake, the major natural process that removes dissolved ions from the brine is mineral precipitation. A comparison between current and 1960 mass of dissolved ions (based on chemical compositions and lake's volume, Table 1 & Table 4), shows that a significant decrease in Na^+ and SO_4^{2-} quantities occurred due to the precipitation of halite and gypsum, respectively. A proportionally smaller decrease was observed for Cl^-, which is due to its relatively high concentrations in comparison to Na^+. Similarly, Ca^{2+} concentration is not sensitive to the precipitation of gypsum because of the high Ca^{2+}/SO_4^{2-} ratio and low precipitation

potential (the maximal amount of gypsum that can precipitate until attainment of equilibrium). Thus, no measurable change is detected in the weight of dissolved Ca^{2+} since 1960. Although anthropogenic induced precipitation of carnellite occurred extensively in the evaporation ponds of the chemical industries since 1960, K^{+} only decreased by ~5% while Mg^{2+}, which has a much higher concentration and is harvested to a lesser extent by the industry has not changed within measurement error (most of the Mg^{2+} that is pumped by the factories is returned to the Dead Sea).

Using the values presented in Table 4, $\sim 36 \cdot 10^{8}$ ton of halite precipitated from the Dead Sea brine between 1960 and 2008. Assuming that this mass is spread homogeneously on the seafloor, it has by now accumulated to a thickness of ~2.5m. Following the same line of reasoning, $20 \cdot 10^{6}$ tons of SO_4^{2-} has precipitated since 1960, resulting in a reduction of ~27% in the mass of dissolved SO_4^{2-} in the lake. If all this mass precipitated as gypsum, $\sim 35 \cdot 10^{6}$ tons of gypsum precipitated on the seafloor, accumulating to a total thickness of only ~2.5 cm, i.e. 2 orders of magnitude less than the halite accumulation. It should however be noted that the above values represent a maximal thicknesses, since some of the Na^{+} and SO_4^{2-} were removed from the brine as gypsum and halite that precipitated in the evaporation ponds of the chemical industries.

The average rate at which SO_4^{2-} concentration decreased between 1960 and 2008 is ~35 μmol kg H_2O^{-1} per year. Thus, in order to detect changes in SO_4^{2-} concentrations in the lake, at least 4 years are required before the change exceeds the range in the analytical error of $\sim \pm 140\ \mu m^{-1}$ (1 standard deviation). Even if the rate of concentration decrease will remain constant over years to come, the quantities of precipitated gypsum are expected to decrease since the Dead Sea volume decreases with time.

Neev and Emery (1967) showed a strong inverse linear relationship between density and SO_4^{2-} concentrations, attained from historic measurements of the Dead Sea brine between the years 1919-1960. This relationship is extended in the present study (Fig. 7) by adding more recent density and chemical data. Data for figures 7-10 consist of several groups: Diluted Dead Sea solutions with a density lower than the current bulk value, Dead Sea values measured between 1980-2008, and end brines which are returned to the Dead Sea after the industrial process is over and serve as a proxy for the future Dead Sea upon its continued evaporation. Several other points were added to the graphs: bulk composition in 1960 (Table 1), upper water mass (UWM) in 1960 and lower water mass (LWM). Since gypsum precipitation has only negligible impact on Ca^{2+} content in the Dead Sea, Ca^{2+} concentrations are proportional to the density of the solution (Fig. 8). As a result, the Ca^{2+}/SO_4^{2-} ratio increases with density (Fig. 9). (Neev, 1964; Neev and Emery, 1967; Gavrieli et al., 1994; Gavrieli, 1997)

As discussed above, the increasing Ca^{2+}/SO_4^{2-} ratio and salinity (in this range of ionic strength) decrease the solubility of gypsum. We showed that according to both theoretical considerations and experimental observations, the kinetics of gypsum nucleation and crystal growth are expected to slow down as the solubility decreases. If the kinetics is indeed slower, it is expected that the Dead Sea brine will be able to retain a higher degree of supersaturation as the brine evaporates further. Indeed, since 1960 (when Ca^{2+}/SO_4^{2-} ratio was 86 and solubility was ~4500 μmol kg H_2O^{-1}) DSG increased from 1.20 to the current value of 1.42 (Ca^{2+}/SO_4^{2-}=115 and solubility ~3200 μm^{-1}). Moreover, Figure 10 shows that as Dead Sea brine becomes more concentrated, DSG increases up to values of 2.75 at a density of ~1.35. The trend shown in figure 10 represents a balance between the increase in DSG due to evaporation and the

decrease in DSG due to precipitation of gypsum. Since the trend strongly depends on the residence time of the system, extrapolation should be carefully considered. Furthermore, if the mechanism of either the nucleation or crystal growth precipitation would change with increasing DSG's, the trend of DSG vs. density may change.

Due to the decrease in the water activity of the brine with increasing salinity, the Dead Sea cannot desiccate completely (Yechieli et al., 1998; Krumgalz et al., 2000). We suggest that DSG will continue to rise as long as the lake experiences negative water balance, volume decrease and an overall salinity increase. Maximum DSG will be reached when a new steady state between inflow and evaporation is attained. From that point in time, DSG values would decrease at a very slow rate, in accordance with precipitation kinetics until the attainment of very close to equilibrium conditions.

5 SUMMARY AND CONCLUSIONS

The kinetics of gypsum nucleation and crystal growth in the Dead Sea brine (DSG=1.42) are slow compared to other solutions with similar degrees of supersaturation. Although precipitation of gypsum occurs in the lake as a result of its constant evaporation, the Dead Sea supersaturation with respect to gypsum increased over the last few decades. Laboratory experiments presented here show that present-day Dead Sea brine can remain supersaturated for a prolonged period of time if no suitable crystallization seeds are available. Although gypsum does nucleate in the Dead Sea, the crystals sink relatively fast through the water column and do not serve as readily available crystallization seeds. Furthermore, the natural flux of clay and carbonate minerals into the lake is insufficient to prompt significant heterogeneous growth of gypsum.

Figure 1 summarized the possible effects of evaporation and consequential precipitation on the precipitation rate of minerals. For the case of the high ionic strength Dead Sea brine, the solubility is low due to a combined effect of high activity coefficients of the free ions (>1) and high Ca^{2+}/SO_4^{2-} ratio (115) which overrides the contradictory effect of aqueous complexes. Adsorption of Na^+ and K^+ (1.5 *m* and 0.2 *m*, respectively, in the Dead Sea brine) onto the gypsum's surface leads to a decrease in precipitation rates as well.

As the Dead Sea will continue to evaporate, gypsum will continue to precipitate from the brine, thereby further increasing the ionic strength and Ca^{2+}/SO_4^{2-} ratio and reducing the solubility. Further evaporation will also lead to higher concentration of inhibiting cations. As the solubility will decrease and inhibitor concentration will increase, both the kinetics of nucleation and crystal growth will slow down, resulting in a solution that will maintain increasingly higher degrees of supersaturation.

Acknowledgments. This research was supported by the Israeli Ministry of National Infrastructure (grants #ES-38-2005 and #ES-28-2006 to JG and IG) and by the Israel Science Foundation (grant #902/05 to IG). I. J Reznik is grateful to the Rieger Foundation – *JNF Program for Environmental Studies* and to the Water Authority of Israel for their generous support. We thank the associate editor, Timothy W. Lyons, for handling the manuscript and for his fruitful comments as well as David Fike and an anonymous reviewer for their thorough review of the manuscript. We wish to express our gratitude to G. Antler, Y. Tubul, T. Feldt and K. Stein for their technical assistance.

Table 1: Average chemical composition of the Dead Sea brine used in the experiments and the Dead Sea composition in 1960 (from Neev and Emery, (1967)) (*m*).

Description	Na^+	K^+	Ca^{2+}	Mg^{2+}	Sr^{2+}	Ba^{2+}	Cl^-	Br^-	SO_4^{2-}	Ca^{2+}/SO_4^{2-}	DSG
Dead Sea 2008	1.5260	0.2275	0.5252	2.1697	0.0046	0.000040	7.2566	0.0717	0.00457	115	1.42±0.11
Dead Sea 1960	1.8809	0.2051	0.4646	1.8791	-	-	6.6171	0.0708	0.00540	86	1.20±0.10

Table 2: Experimental conditions and results of flow-through experiments

Exp.	Seeding material	Seeding (g)	Flow rate (g min^{-1})	[1]ρ (g cm^{-3})	SO_4 (inflow) µmol kg^{-1}	SO_4 (outflow) µmol kg^{-1}	[2]Δ Sulfate µmol kg^{-1} ±error	Rate*1e^{10} (mol m^{-2} s^{-1})	Rate*1e^{10} (mol s^{-1})	Duration of steady state (days)	[3]n
AN	Gypsum	2	0.106	1.238	2994	2474	520±23	10	9.2	26.1	26
AO	None	0	0.113	1.239	2932	2948	-16±27	-	-	32.4	21
AP	Gypsum	0.5	0.072	1.239	3197	2473	725±23	27	8.6	42.0	27
AQ	Gypsum	1	0.051	1.240	3400	2514	886±57	17	7.4	7.0	5
AR	Montmorilonite	0.5	0.064	1.240	3250	3238	12±56	-	-	7.8	6
AS	Kaolinite	0.5	0.077	1.240	3250	3263	-13±49	-	-	14.0	8
AT	Gypsum	0.1	0.072	1.240	3195	2702	493±51	100	5.9	8.9	6
AU	Gypsum	0.0011	0.094	1.239	3237	3182	55±45	292	0.9	5.7	9
AV	Gypsum	0.01	0.099	1.239	3237	2955	282±59	185	4.6	5.8	5
BJ	Aragonite	0.5	0.108	1.240	3140	3116	24±38	-	-	13.1	12
BK	Calcite	0.5	0.106	1.241	3167	3154	13±29	-	-	20.8	21

[1]ρ=density; [2]error for $\Delta_{sulfate}$ was calculated based on the SO_4^{2-} analytical error and number of samples at SS ($3\%/n^{1/2}$), [3]n = number of samples at steady state.

Table 3: Experimental conditions and results of batch experiments

Seeding Material	Seeding (g)	DS weight (g)	Initial SO_4^{2-} concentration ($\mu mol\ kg^{-1}$)	Final SO_4^{2-} concentration ($\mu mol\ kg^{-1}$)	$\Delta\ SO_4^{2-}$ concentration ($\mu mol\ kg^{-1}$)	Initial DSG	Final DSG
Aragonite	1.0255	58.889	3007	2707	300	1.36	1.19
Calcite	0.9924	58.846	3007	2873	134	1.36	1.27
Montmorilonite	0.9943	59.117	3007	2885	122	1.36	1.27
Kaolinite	1.0037	58.997	3007	2951	56	1.36	1.30
Gypsum	1.0087	58.905	3007	2279	728	1.36	1.00
Control	0	59.967	3007	2970	37	1.36	1.31

Table 4 : Masses of dissolved ions in Dead Sea brine

(Tons x 10^9)

Description	Na^+	K^+	Ca^{2+}	Mg^{2+}	Cl^-	Br^-	SO_4^{2-}	Volume (km^3)
Dead Sea 2008	4.1	1.04	2.46	6.15	30.0	0.67	0.051	130
Dead Sea 1960	5.9	1.09	2.53	6.20	31.9	0.77	0.071	148
Difference 1960-2008	1.8±0.1	0.05±0.03	0.074±0.074	0.05±0.18	1.9±0.9	0.1±0.02	0.019±0.002	
Decrease since 1960	30%	5%	no change	no change	6%	13%	27%	12%

6 FIGURE CAPTIONS

Fig. 1 Schematic illustration of the effects of evaporation and mineral precipitation on chemical parameters of the solution and the consequent impact on the precipitation kinetics. A "+" sign denotes an increase of a parameter (e.g., "R+" denotes an increase in precipitation rate), while a "-" sign denotes a decrease of it. See the legend for details.

Fig. 2 Flow-through experimental setup.

Fig. 3 Inflow and outflow SO_4^{2-} concentrations over time in flow-through experiments conducted with gypsum crystallization seeds (experiment AN) and with no crystallization seeds (experiment AO).

Fig. 4 SO_4^{2-} concentrations as a function of time in batch experiments containing different seeding material. The solid line represents the initial SO_4^{2-} concentration for all experiments.

Fig. 5 The effect of deviation from equilibrium on precipitation rates of gypsum (mol m^{-2} s^{-1}) in flow-through experiments with Dead Sea brine.

Fig. 6 The effect of Ca^{2+}/SO_4^{2-} molar ratio on gypsum precipitation rate. Most of the data (squares) are from Zhang and Nancollas, (1992). The curve was fitted only for these points. The datum for the Dead Sea brine (triangle) is from the present study. All the rate data are corrected to DSG of 1.69.

Fig. 7 Inverse linear relationship between SO_4^{2-} concentrations and density in Dead Sea brines and their derivatives. UWM and LWM stand for the 1960 upper and lower Dead Sea water masses, respectively.

Fig. 8 Ca^{2+} concentrations vs. density of Dead Sea brines and their derivatives.

Fig. 9 Ca^{2+}/SO_4^{2-} ratio vs. density in Dead Sea brines and their derivatives.

Fig. 10 DSG vs. density in Dead Sea brines and their derivatives.

7 REFERENCES

Alimi, F. and Gadri, A., (2004). Kinetics and morphology of formed gypsum. *Desalination* **166**, 427-434.

Amjad, Z., (1985). Applications of antiscalants to control calcium sulfate scaling in reverse osmosis systems. *Desalination* **54**, 263-276.

Billo, S. M., (1986). Petrology and kinetics of Gypsum-Anhydrite transitions. *Journal of Petroleum Geology* **10**, 73-86.

Bosbach, D., Junta-Rosso, J. L., Becker, U., and Hochella, M. F., (1996). Gypsum growth in the presence of background electrolytes studied by Scanning Force Microscopy. *Geochimica et Cosmochimica Acta* **60**, 3295-3304.

Bosbach, D. and Rammensee, W., (1994). In situ investigation of growth and dissolution on the (010) surface of gypsum by Scanning Force Microscopy. *Geochimica et Cosmochimica Acta* **58**, 843-849.

Brandse, W. P., Vanrosmalen, G. M., and Brouwer, G., (1977). The influence of sodium-chloride on crystallization rate of gypsum. *Journal of Inorganic and Nuclear Chemistry* **39**, 2007-2010.

Brunauer, S., Emmett, P. H., and Teller, E., (1938). Adsorption of gases in multimolecular layers. *Journal of American Chemical Society* **60**, 309-319.

Burton, W. K., Cabrera, N., and Frank, F. C., (1951). The growth of crystals and the equilibrium structure of their surfaces. *Philosophical Transactions of the Royal Society London* **243**, 299-358.

Christoffersen, M. R., Christoffersen, J., Weijnen, M. P. C., and Van Rosmalen, G. M., (1982). Crystal growth of calcium sulphate dihydrate at low supersaturation. *Journal of Crystal Growth* **58**, 585-595.

Cody, A. M. and Cody, R. D., (1989). SEM and polarization analyzes updating early light microscope studies related to {101} twin formation in gypsum. *Journal of Crystal Growth* **98**, 731-738.

Deutsch, Y., Nathan, Y. Sarig, S., (1994). Thermogravimetric evaluation of the kinetics of the Gypsum-hemihydrate- soluble anhydrate transitions. *Journal of Thermal Analysis* **42**, 159-174.

Edinger, S. E., (1973). An investigation of the factors which affect the size and growth rates of the habit faces of gypsum. *Journal of Crystal Growth* **18**, 217-224.

El-Shall., H., Rashad., M. M., and Abdel-Aal., E. A., (2002). Effect of Phosphonate Additive on Crystallization of Gypsum in Phosphoric and Sulfuric Acid Medium. *Cryst. Res. Technol.* **37**, 1264-1273.

Gavrieli, I., (1997). Halite Deposition from the Dead Sea: 1960-1993. In: Niemi, T. M., Ben-Avraham, Z., Gat, J.R (Ed.), *The Dead Sea - the lake and its setting*, Oxford University Press, New York oxford.

Gavrieli, I., Beyth, M., Weinstein, R., and Anati, D. A., (1994). The effect of the decrease in the stability of the Dead Sea water column stratification on the mixing mechanism of the End Brines in the southern Dead Sea. Geological Survey of Israel, Jerusalem, p.

Gavrieli, I., Oren A., (2004). The Dead Sea as a Dying Lake. In: C.J, N. J. and O., Z. P. (Eds.), *Dying and Dead Seas Climatic Versus Anthropic Causes*, IV. Earth and Environmental Sciences. Kluwer Academic Publishers, Kalamazoo.

Gill, J. S. and Nancollas, G. H., (1979). The growth of gypsum crystals on barite and calcite. *Desalination* **29**, 247-254.

Goto, M. and Ridge, M. J., (1967). Crystal Growth of Gypsum on its Cleaved Surface. *J.Fac. Sci.* **4**, 349-382.

Hall, C. and Cullen, D., (1996). Scanning Force Microscopy of Gypsum Dissolution and Crystal Growth. *AIChE Journal* **42**, 232-238.

He, S., Oddo, J. E., and Tomson, M. B., (1994a). The Nucleation Kinetics of Calcium Sulfate Dihydrate in NaCl Solutions up to 6 m and 90°C. *Journal of Colloid and Interface Science* **162**, 297-303.

He, S., Oddo, J. E., and Tomson, M. B., (1994b). The Seeded Growth of Calcium Sulfate Dihydrate Crystals in NaCl Solutions up to 6 m and 90ºC. *Journal of Colloid and Interface Science* **163**, 372-378.

Herut, B., Gavrieli, I., and Halicz, L., (1998). Coprecipitation of trace and minor elements in modern authigenic halites from the hypersaline Dead Sea brine. *Geochimica et Cosmochimica Acta* **62**, 1587-1598.

Kagawa, M., Sheehan, M. E., and Nancollas, G. H., (1981). The crystal growth of gypsum in an ammoniacal environment. *Journal of Inorganic and Nuclear Chemistry* **43**, 917-920.

Katz, A., Starinsky, A., Taitel-Goldman, N., and Beyth, M., (1981). Solubilities of Gypsum and Halite in the Dead Sea and in Its Mixtures with Seawater. *Limnology and Oceanography* **26**, 709-716.

Krumgalz, B. S., (1997). Ion interaction apporch to geochemical aspects of the Dead Sea. In: Niemi, T. M., Ben-Avraham, Z., Gat, J.R (Ed.), *The Dead Sea - the lake and its setting*, Oxford University Press, New York oxford.

Krumgalz, B. S., (2001). Application of the Pitzer ion interaction model to natural hypersaline brines. *J. Molecular Liquids* **91**, 3-19.

Krumgalz, B. S., Hecht, A., Starinsky, A., and Katz, A., (2000). Thermodynamic constraints on Dead Sea evaporation: can the Dead Sea dry up? *Chemical Geology* **165**, 1.

Krumgalz, B. S. and Millero, F. J., (1982). Physico-Chemical Study of the Dead Sea Waters. I. Activity Coefficients of Major Ions in Dead Sea Water. *Marine Chemistry* **11**, 209-222.

Krumgalz, B. S. and Millero, F. J., (1983). Physico-Chemical Study of the Dead Sea Waters. III. On gypsum saturation in Dead Sea waters and their mixtures with Mediterranean Sea Water. *Marine Chemistry* **13**, 127-139.

Lancia, A., Musmarra, D., and Marina, P., (1999). Measuring Induction Period for Calcium Sulfate Dihydrate Precipitation. *AIChE Journal* **45**, 390-397.

Lasaga, A. C., (1998). *Kinetic Theory in the Earth Sciences*. Princeton University Press, Princeton, NJ.

Levy, Y., (1987). The Dead Sea - Hydrographic, Geochemical and Sedimentological changes during the last 25 years (1959-1984). Geological Survey of Israel, Jerusalem, p.

Liu, S.-T. and Nancollas, G. H., (1970). The kinetics of crystal growth of calcium sulfate dihydrate. *Journal of Crystal Growth* **6**, 281-289.

Liu, S.-T. and Nancollas, G. H., (1973). Linear crystallization and induction-period studies of the growth of calcium sulphate dihydrate crystals. *Talanta* **20**, 211-216.

Metz, V., Amram, K., and Ganor, J., (2005). Stoichiometry of smectite dissolution reaction. *Geochimica et Cosmochimica Acta* **69**, 1755-1772.

Nancollas, G. H., (1979). The growth of crystals in solution. *Advances in Colloid and Interface Science* **10**, 215-252.

Neev, D., (1964). *The Dead Sea*. The Geological Survey of Israel, Jerusalem.

Neev, D. and Emery, K. O., (1967). The Dead Sea - Depositional processes and environments of evaporites. Minisrty of Development - Geological Survery of Israel, Jerusalem, 147 p.

Nielsen, A. E., (1981). Theory of Electrolyte Crystal Growth - The Parabolic Rate Law. *Pure & appl. Chem.* **53**, 2025-2039.

Nielsen, A. E. and Sohnel, O., (1971). Interfacial tensions electrolyte crystal-aqueous solution, from nucleation data. *Journal of Crystal Growth* **11**, 233-242.

Packter, A., (1974). The precipitation of calcium sulphate dihydrate from aqueous solution : Induction periods, crystal numbers and final size. *Journal of Crystal Growth* **21**, 191-194.

Parkhurst, D. L. and Appelo, C. A. J., (2007). PHREEQC 2.14.3 A computer program for speciation, batch-reaction, one-dimentional transport and inverse geochemical calculation. *Water- Resources Investigation Report 99-4259*. U.S. Geological Survey., p.

Pruett, R. J. and Webb, H. L., (1993). Sampling and analysis of KGa-1B well crystallized kaolin source clay. *Clays and Clay Minerals* **41**, 514-519.

Reznik , I. J., Gal, A., Ganor, J., and Gavrieli, I., (2009). Gypsum saturation degrees and precipitation potential from Dead Sea-Seawater mixtures - Implication for the Red Sea - Dead Sea Conduit. *Environmental Chemistry* **submitted**.

Sheikholeslami, R. and Ong, H. W. K., (2003). Kinetics and thermodynamics of calcium carbonate and calcium sulfate at salinities up to 1.5 M. *Desalination* **157**, 217-234.

Smith, B. R. and Sweett, F., (1971). The crystallization of calcium sulfate dihydrate. *Journal of Colloid and Interface Science* **37**, 612-618.

Sohnel, O., (1982). Electrolyte crystal-aqueous solution interfacial tensions from crystallization data. *Journal of Crystal Growth* **57**, 101-108.

Stein, M., Starinsky, A., Katz, A., Goldstein, S. L., Machlus, M., and Schramm, A., (1997). Strontium isotopic, chemical, and sedimentological evidence for the evolution of Lake Lisan and the Dead Sea. *Geochimica et Cosmochimica Acta* **61**, 3975-3992.

Steinhorn, I., (1983). In situ salt precipitation at the Dead Sea. *Limnology and Oceanography* **28**, 580-583.

Torfstein, A., Gavrieli, I., Katz, A., Kolodny, Y., and Stein, M., (2008). Gypsum as a monitor of the paleo-limnological-hydrological conditions in Lake Lisan and the Dead Sea. *Geochimica et Cosmochimica Acta* **72**, 2491.

Van Rosmalen, G. M., Daudey, P. J., and Marchee, W. G. J., (1981). An analysis of growth experiments of gypsum crystals in suspension. *Journal of Crystal Growth* **52**, 801-811.

Witkamp, G. J., Van der Eerden, J. P., and Van Rosmalen, G. M., (1990). Growth of gypsum : I. Kinetics. *Journal of Crystal Growth* **102**, 281-289.

Yechieli, Y., Gavrieli, I., Berkowitz, B., and Ronen, D., (1998). Will the Dead Sea die? *Geology* **26**, 755-758.

Zhang, J. and Nancollas, G. H., (1992). Influence of calcium/sulfate molar ratio on the growth rate of calcium sulfate dihydrate at constant supersaturation. *Journal of Crystal Growth* **118**, 287-294.

Reznik et al., Fig. 1

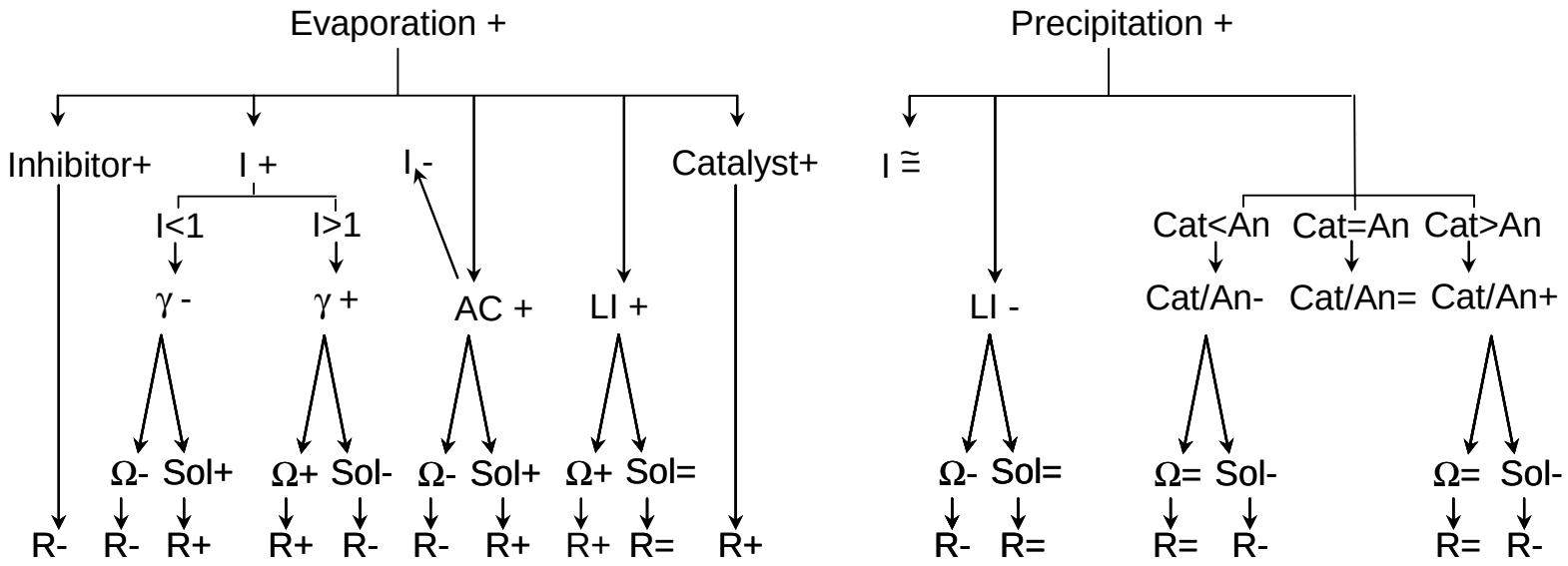

Legend:

"+"=increase of value; "-"=decrease of value; "="= no change; I=ionic strength; γ=activity coefficients; AC=aqueous complexes; LI=concentration of lattice ions; Cat=lattice cation activity; An=lattice anion activity; Ω=degree of saturation; Sol=solubility; R=precipitation rate

Reznik et al., Fig. 2

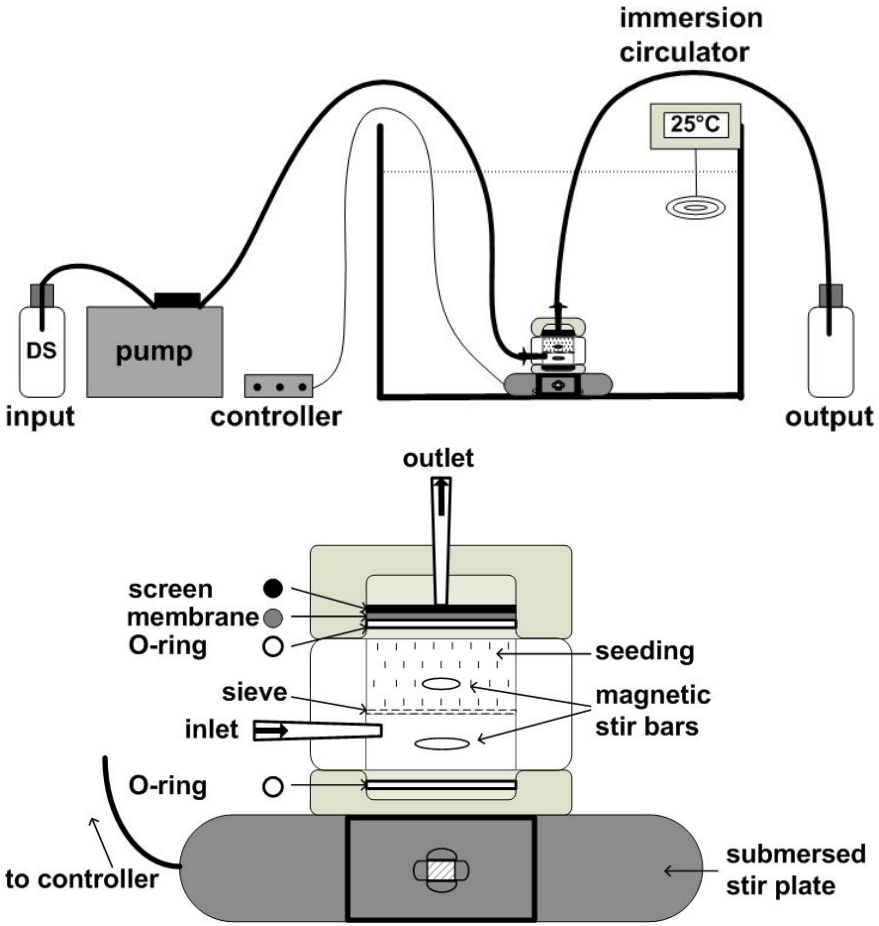

Reznik et al., Fig. 3

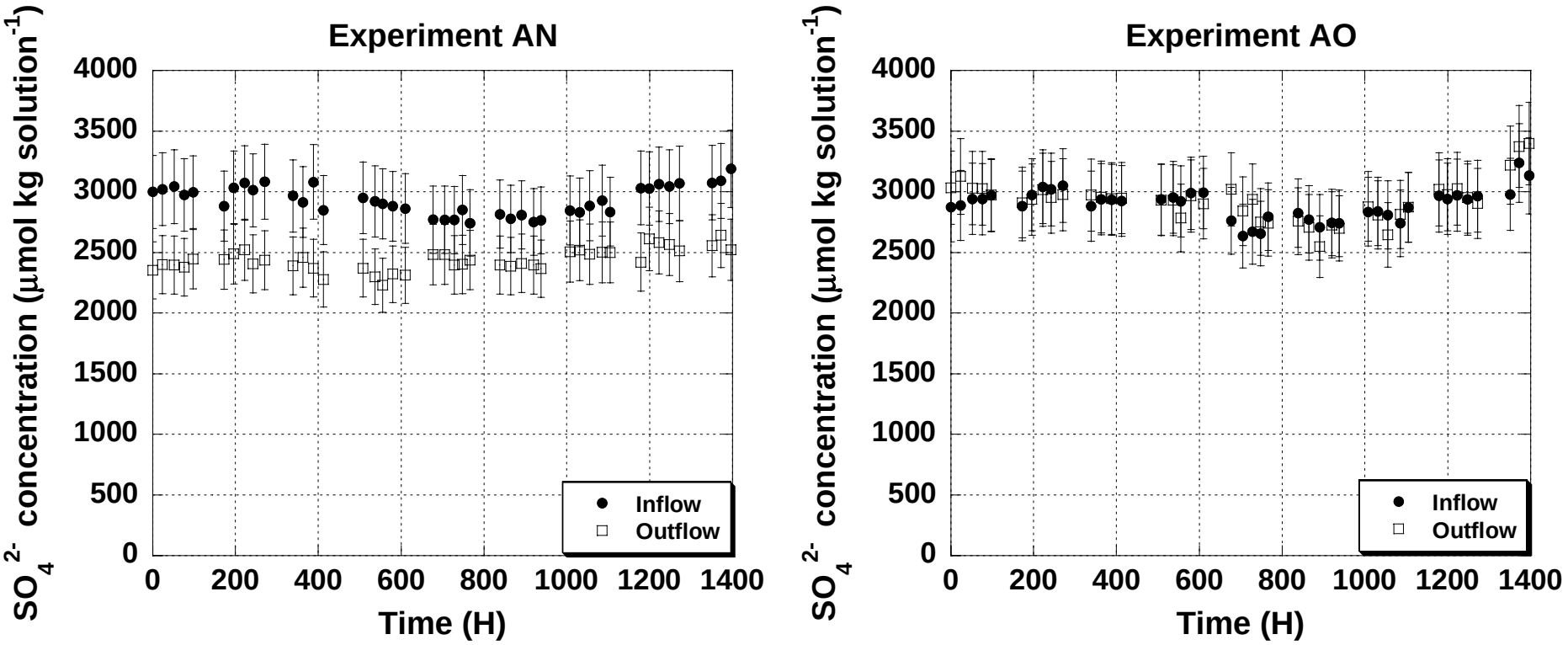

Reznik et al., Fig. 4

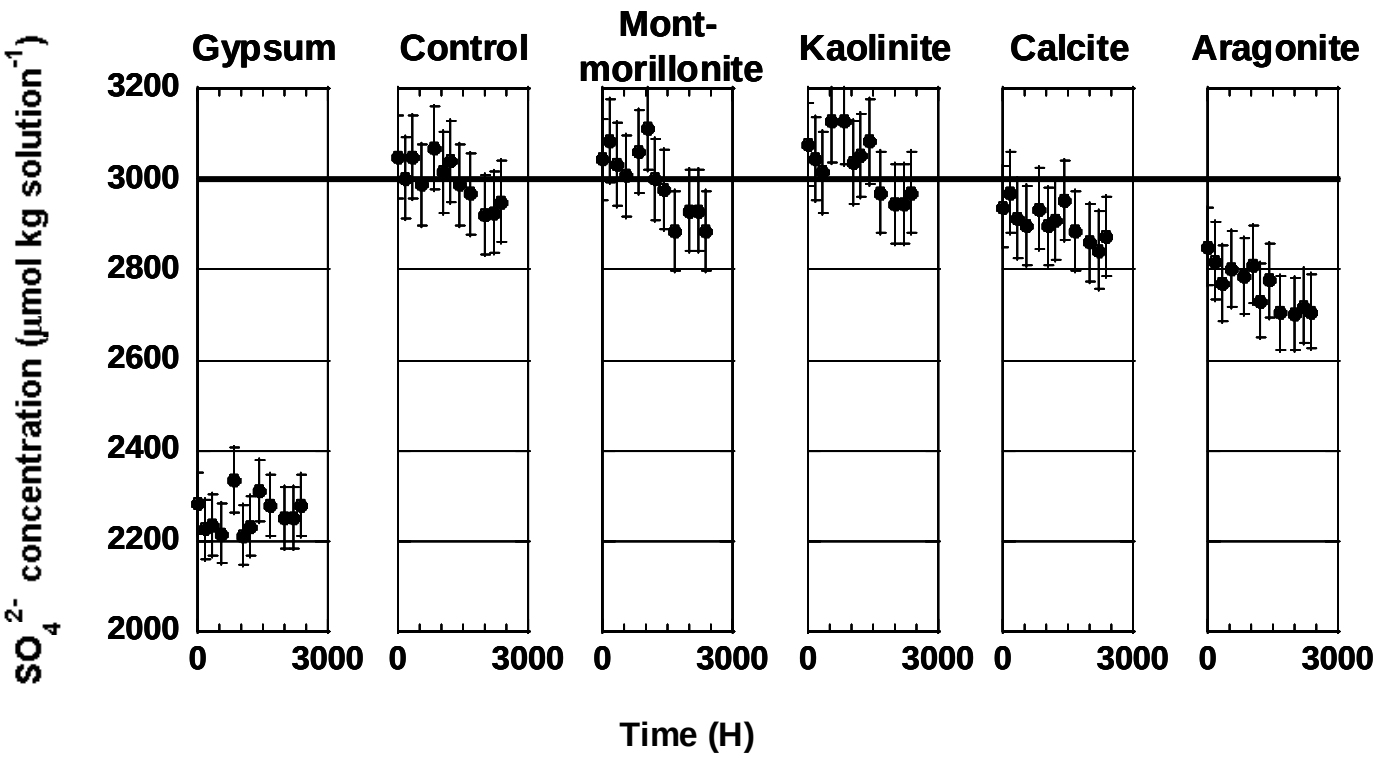

Reznik et al., Fig. 5

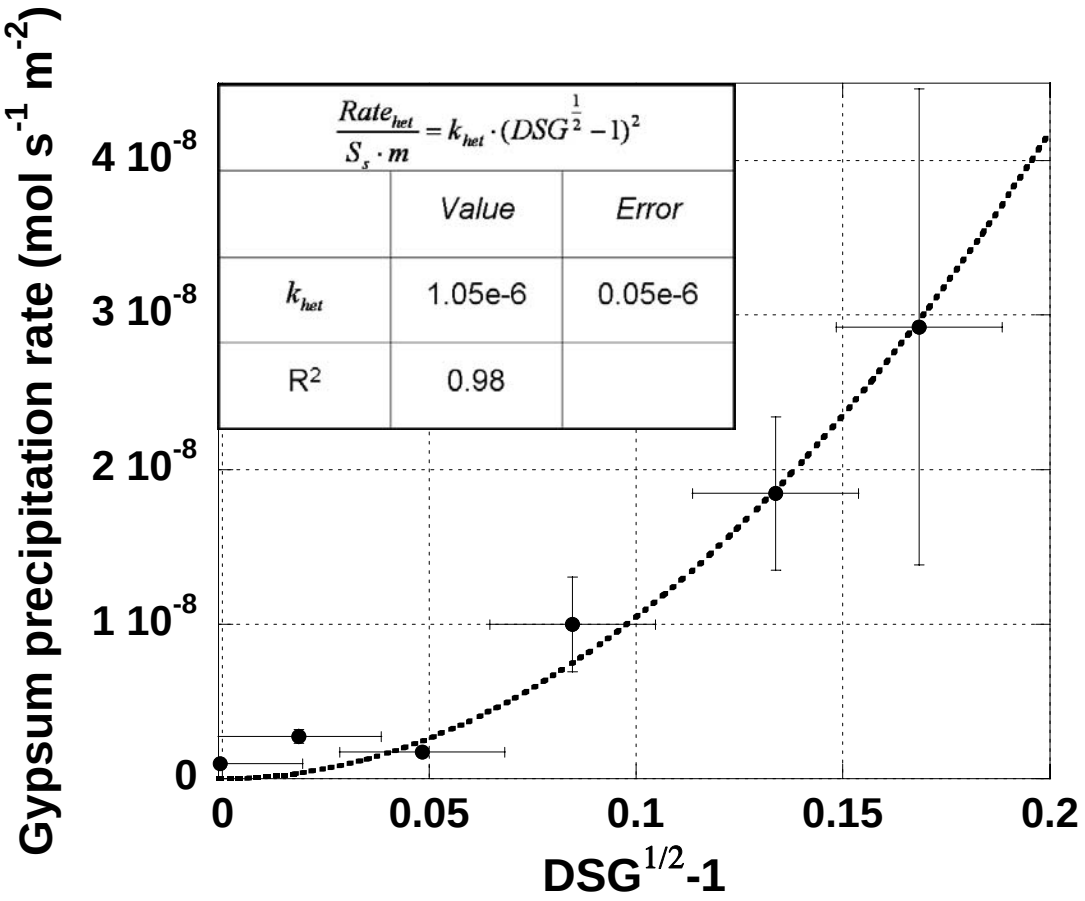

Reznik et al., Fig. 6

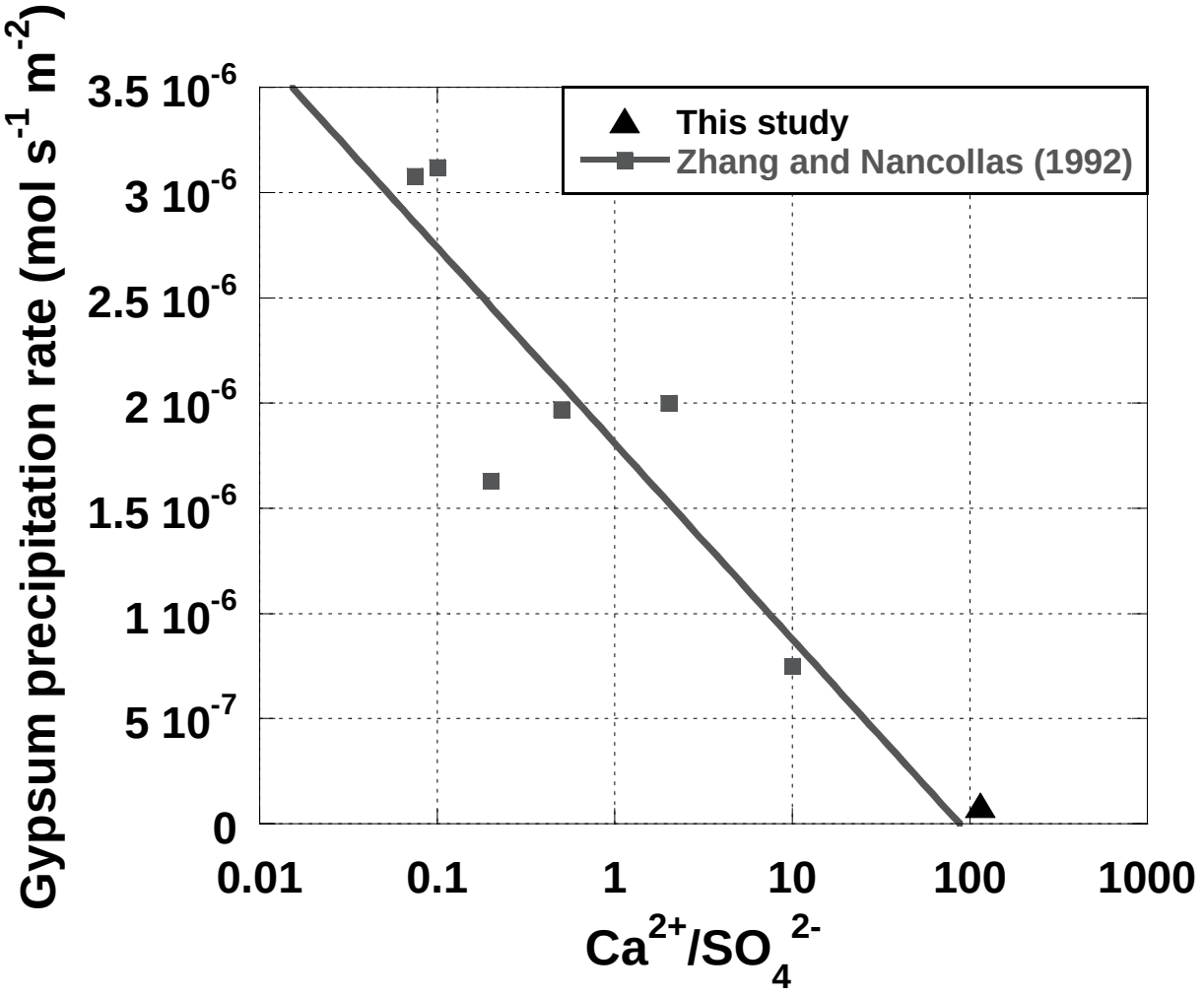

Reznik et al., Fig. 7

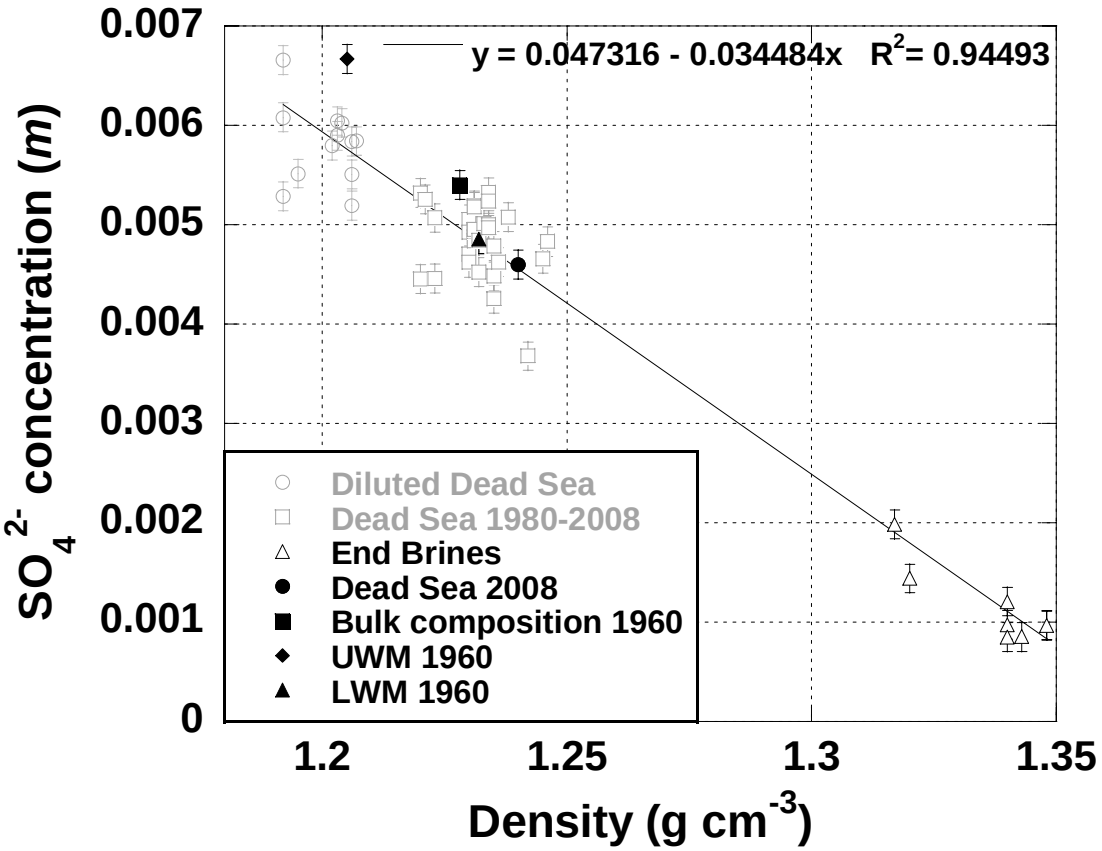

Reznik et al., Fig. 8

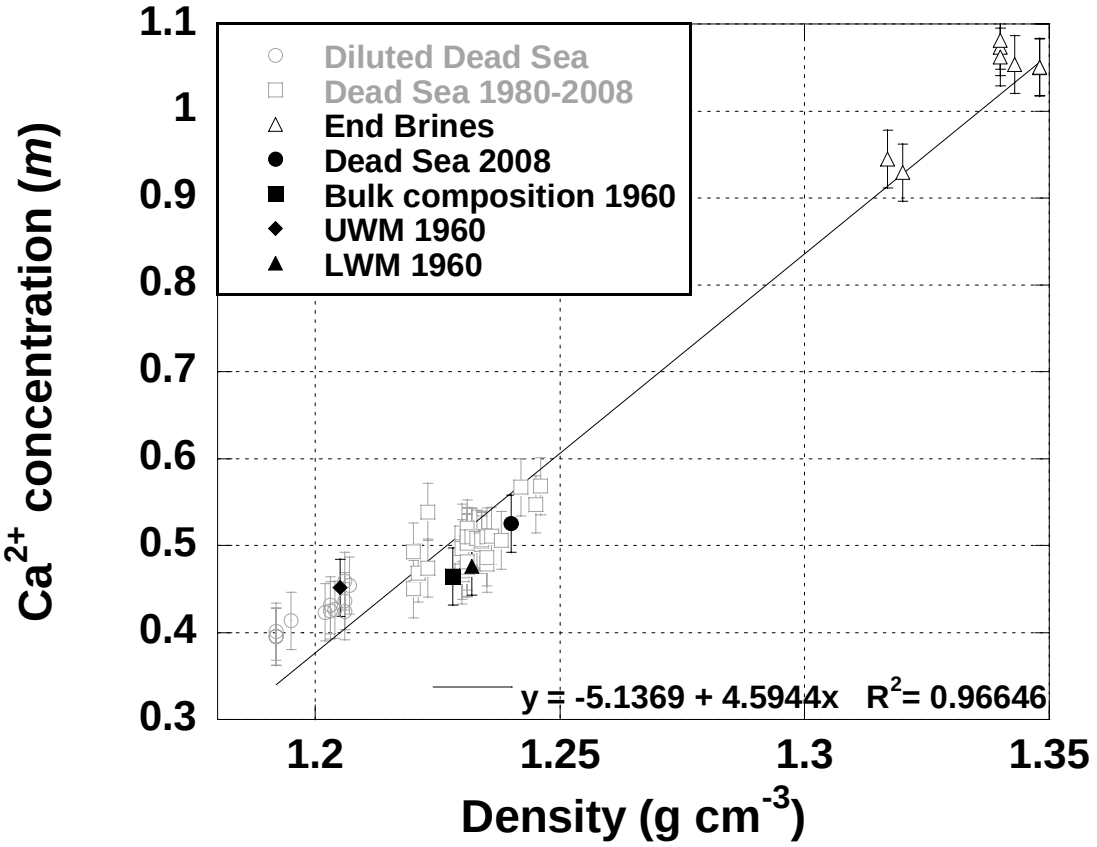

Reznik et al., Fig. 9

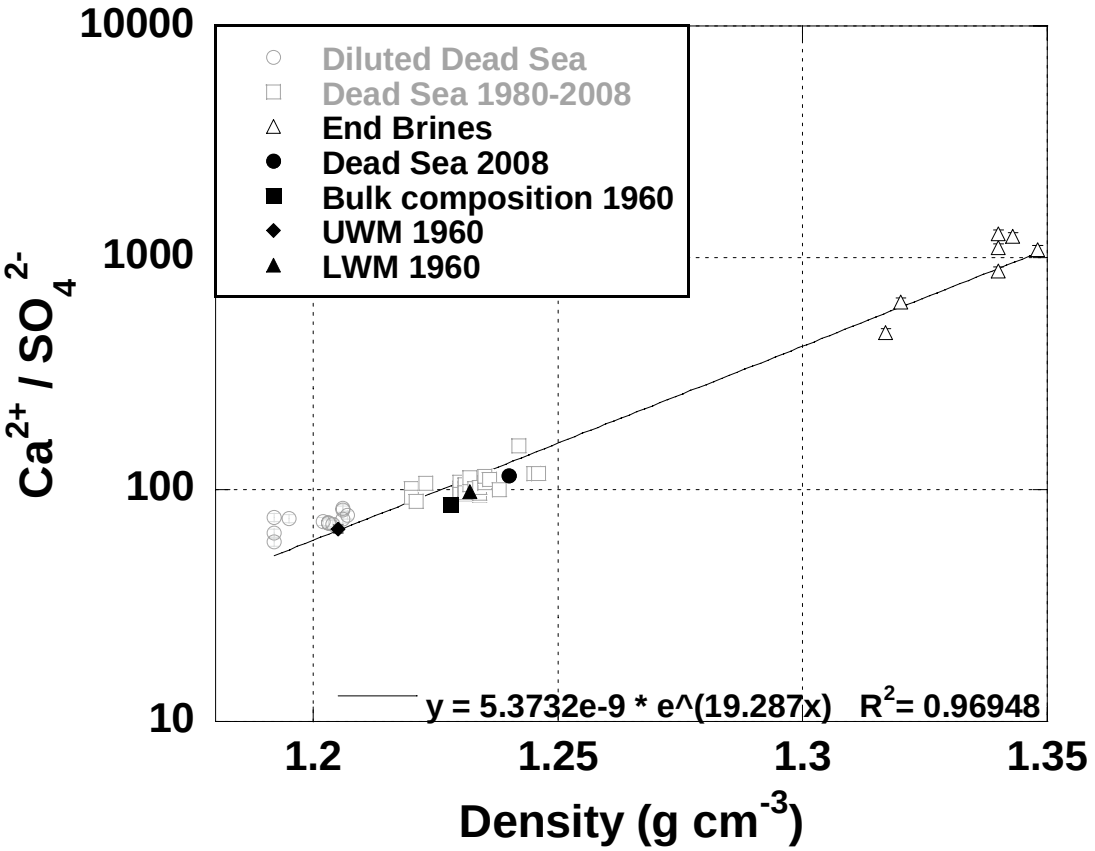

Reznik et al., Fig. 10